Silsesquioxane Barrier Materials

Michael Z. Asuncion[†] and Richard M. Laine*[,†,‡]

Department of Materials Science and Engineering and Macromolecular Science and Engineering Center, University of Michigan, Ann Arbor, Michigan 48109-2136

Received October 5, 2006; Revised Manuscript Received November 21, 2006

ABSTRACT: Cubic octameric silsesquioxanes, because of their octahedral structures and nanometer size, represent potentially very useful nanoconstruction sites. Here we report the reaction of octaaminophenylsilsesquioxane (OAPS) with a variety of epoxides and dianhydrides and their subsequent heat treatment to form nanocomposite films with exceptional oxygen barrier properties. While solution-cast films give relatively low oxygen transmission rates (OTR), casting followed by warm-pressing lowers the OTR to values competitive with commercially available high-performance barrier films. The lowest OTR measured was obtained with a warm-pressed bilayer films consisting of OAPS/tetraglycidyl-*m*-xylenediamine and OAPS/2,4-epoxycyclohexylmethyl-3,4-epoxycyclohexanecarboxylate with OTRs < 1 cm^3 20 $\mu m/(m^2$ day atm). These silsesquioxane films are thermally very robust, particularly the OAPS/imide films (>500 °C when fully cured), making them ideal for electronics packaging and encapsulation applications.

Introduction

One of the oft-repeated objectives of nanoscience and nanotechnology is to develop methods of constructing materials from the bottom up. However, the potential to realize such approaches is limited by the availability of building blocks that permit the strategic design of materials and thereafter their construction with nanometer by nanometer control. The literature is replete with articles on the design and synthesis of nanosized particles and their assembly to nanostructured materials;[1−6] however, there are very few building blocks that offer the potential for nanometer by nanometer construction in 1-, 2-, or 3-D with control of periodicity over millimeter and even centimeter length scales and therefore global properties.

Octasilsesquioxanes,[7−11] $Q_8[RMe_2SiOSiO_{1.5}]_8$ and $T_8[RSiO_{1.5}]_8$ (R = alkyl, alkenyl, alkynyl, aryl, epoxy, methacrylate, aromatic, etc.; Figure 1), are spherical molecules ≈1.0 nm in diameter with cubic symmetry that places a functional group in each octant in Cartesian space, thereby, in principle, permitting their assembly one nanometer at a time in 1-, 2-, or 3-D with complete control of periodicity. In principle, through control of the architecture of the organic groups connecting the vertices of each silsesquioxane, it is possible to tailor global properties.

We and others have begun to explore their utility for building nanostructured materials, nanocomposites for diverse applications.[12−30] Our initial goal was first to prove that it is possible to both assemble Q_8 and T_8 systems in 3-D covalently linked nanocomposite networks with precise control of the periodicity over extended length scales.[15,20] A second goal was to demonstrate the potential to tailor global properties through control of the architecture of the organic tethers joining silsesquioxane cage vertices. Our efforts on this emphasis relied on the epoxy and imide chemistries of the Q_8 and T_8 systems, as suggested by reactions 1 and 2 of Scheme 1.[18,19]

One major finding of this work was that traditional epoxy resin stoichiometries, wherein one $-NH_2$ group is reacted with two epoxy moieties ($N = 0.5$), offer poorer mechanical properties than a 1:1 NH_2:epoxy stoichiometry ($N = 1$). In this regard, we recently reported the development of simple, low-viscosity epoxy resins with control of coefficients of thermal expansion (CTEs) over on order of magnitude from 25 to 240 ppm/°C.[22] In an extension of these efforts, we report here that it is possible to use nanometer tailoring of the structures of epoxy and imide systems to produce oxygen barrier films that, unoptimized, are equivalent to those produced commercially while offering improved thermal stability.

At the molecular level, transport of gas molecules across membranes is controlled (1) by the solubility of the gas within the membrane materials followed by diffusion through it[31,32] and (2) the ability to diffuse through the membrane without dissolution via adventitious pores and free volume.[33] Thus, all efforts to make barrier materials must also consider ways of blocking these transport mechanisms.

A review of the literature indicates that superior barrier properties are obtained from polymeric materials modified using an assortment of approaches.[32−39] For example, good barrier properties extend from polymers with strong intrachain forces that induce high packing densities that in turn hinder gas diffusion. Thus, strong hydrogen bonding, chain alignment by extrusion, and high degrees of crystallinity or liquid crystallinity provide one approach to defeating diffusion of gases. Another approach is to add easily dispersed second phases that can be organic or inorganic inclusions such as exfoliated clay particles or simply silica.[39] An extension of this approach is to make bilayer films where transport across the interface is problematic. In the extreme, this can include introduction of an inorganic phase including aluminum (metallized layers). Clearly, the need to disperse or coat a second phase adds to the difficulty and expense of processing as does extrusion or other processing methods that align polymer chains.

If the claim that silsesquioxanes offer tailorability of global properties by assembly at nanometer length scales is to be justified, then it should be possible to develop low-viscosity, single-phase silsesquioxane systems that on curing offer good O_2 transport barrier properties. We describe here our efforts to identify useful barrier systems. It is important to note that the systems developed here also offer considerable potential for modifying CTEs, and abrasion and corrosion resistance.[22]

[†] Department of Materials Science and Engineering.
[‡] Macromolecular Science and Engineering Center.

10.1021/ma062305p CCC: $37.00
Published on Web 01/04/2007

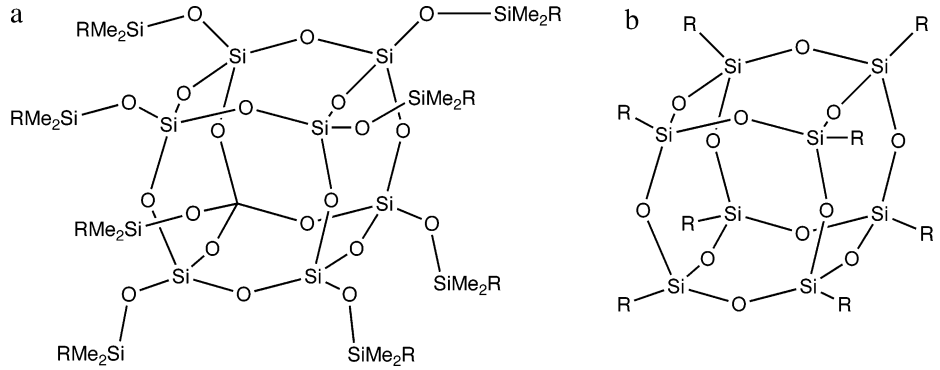

Figure 1. Typical (a) Q_8 and (b) T_8 structures.

Experimental Section

Materials. Tetraglycidyl-*m*-xylenediamine (TGMX, MW 332.4), a gift from Dr. Rafil Basheer of Delphi Corp., and diglycidyl ether of bisphenol A (DGEBA, MW 340.4, Aldrich) were used as received. Standard concentrations of O_2 in helium were purchased from Cryogenic Gases (Detroit, MI). Nano-δ-alumina was received as a gift from from Degussa Inc. and used as received. 4-Vinyl-1-cyclohexene (MW 108.2), pyromellitic dianhydride (PMDA, MW 218.1), 4,4′-oxidianiline (ODA, MW 200.2), 4,4′-oxidiphthalic anhydride (ODPA, MW 310.2), 3,4-epoxycyclohexylmethyl-3,4-epoxycyclohexanecarboxylate (ECHX, MW 252.3), resorcinol digylcidyl ether (RDGE, MW 222.2), and *N*-methylpyrrolidinone (NMP) were purchased from Aldrich (Milwaukee, WI) and used without further purification. Octahydridosilsesquioxane (OHS, MW 1018.0) and octaaminophenylsilsesquioxane (OAPS, MW $\approx$ 1153) were synthesized following methods described in the literature.[16,17] All work was performed under nitrogen.

Analytical Methods. *NMR Analyses*. All ^{1}H NMR analyses were done in $CDCl_3$ and recorded on a Varian INOVA 300 spectrometer. ^{1}H NMR spectra were collected at 300.0 MHz using a 6000 Hz spectral width, a relaxation delay of 3.5 s, a pulse width of 38°, 30K data points, and $CHCl_3$ (7.259 ppm) as an internal reference.

Thermal Gravimetric Analysis (TGA). Thermal stabilities of materials under N_2 or air were examined using a 2960 simultaneous DTA-TGA Instrument (TA Instruments, Inc., New Castle, DE). Samples (5−10 mg) were loaded in platinum pans and ramped to 1000 °C (10 °C/min/N_2). The N_2 or air flow rate was 60 mL/min.

FTIR Spectra. Diffuse reflectance Fourier transform (DRIFT) spectra were recorded on a Mattson Galaxy Series FTIR 3000 spectrometer (Mattson Instruments, Inc., Madison, WI). Optical grade, random cuttings of KBr (International Crystal Laboratories, Garfield, NJ) were ground, with 1.0 wt % of the sample to be analyzed. For DRIFT analysis, samples were packed firmly and leveled off at the upper edge to provide a smooth surface. The FTIR sample chamber was flushed continuously with N_2 prior to data acquisition in the range 4000−400 cm^{-1}.

Curing and Pressing Studies. All samples were cast in round 100 mm diameter Teflon Petri dishes. They were heated in a Thelco laboratory oven (equipped with temperature controller) according to the conditions described in Tables 1 and 2. Heat-pressed samples were precured and subsequently removed from the molds, sandwiched between aluminum foil sheets, and warm-pressed in air according to the conditions described in Table 2**,** from 0.690−1.03 MPa (100−150 psi) in a Carver press model 3851-0 (equipped with heating platens and temperature controller) according to the conditions specified in Table 2. Resulting warm-pressed samples were ∼200 mm in diameter.

OTR Measurements. OTR values were measured using an HP model 5890 series 2 GC equipped with permeation cell and calibrated with 2%, 5%, and 10% concentrations of O_2 in helium. A schematic of the components needed to determine OTR by permeation cell and GC is shown in Figure 2. Test films were cut and mounted (with typical commercial two-part epoxy adhesive) on circular aluminum foil holders 100 mm diameter with circular

Scheme 1

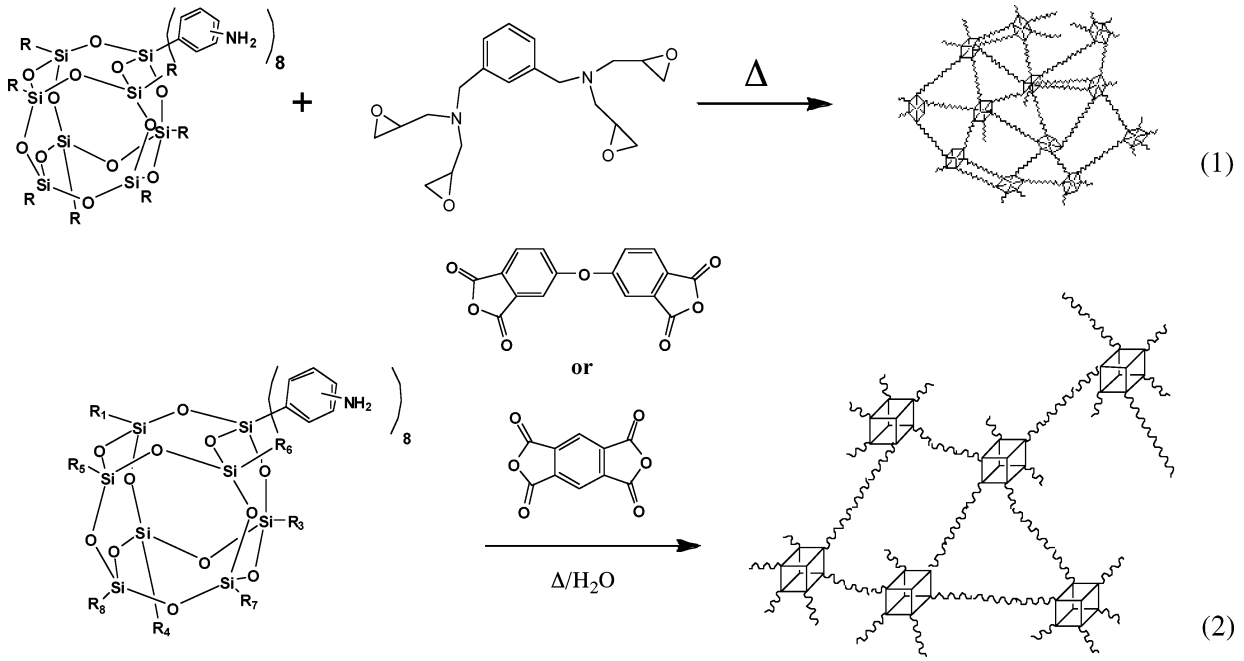

Table 1. Oxygen Transmission Rates (OTR) of Cast Silsesquioxane Films [at 20 °C and 65% RH; cm³ 20 μm/(m² day atm O_2), i.e. Standardized to 20 μm Thickness]

sample	*N* NH_2 groups:epoxide groups	curing	OTR (±0.5) (cm³ 20 μm/(m² day atm))
TCHS [Pt(dcp)]		170 °C/5 h	24000
TCHS (PtO_2)		130 °C/6 h, 130 °C/8 h, 150 °C/8 h, 170 °C/8 h	13000
50% OAPS/PMDA		120 °C/4 h, 205 °C/4 h, 215 °C/4 h	31
50% OAPS/PMDA		120 °C/4 h, 205 °C/4 h, 215 °C/8 h, 240 °C/8	27
50% OAPS/ODPA		120 °C/4 h, 205 °C/4 h	35
50% OAPS/ODPA		120 °C/4 h, 205 °C/4 h, 215 °C/8 h, 225 °C/8 h	25
50% OAPS/ODPA		120 °C/4 h, 205 °C/4 h, 215 °C/8 h, 240 °C/8 h	27
50%OAPS/ODPA/ODA		120 °C/4 h, 205 °C/4 h, 215 °C/8 h, 225 °C/8 h	29
OAPS/DGEBA	0.5	130 °C/5 h	110
OAPS/DGEBA	0.5	130 °C/5 h, 150 °C/5 h	21
OAPS/DGEBA	1.0	130 °C/5 h, 150 °C/5 h	24
OAPS/TGMX	0.5	90 °C/2 h	14
OAPS/ECHX	0.5	100 °C/1 h, 130 °C/4 h	8
OAPS/ECHX	1.0	100 °C/1 h, 130 °C/4 h	24
OAPS/ECHX	0.5	100 °C/1 h, 130 °C/4 h, 180 °C/4 h	6
OAPS/RDGE	0.5	95 °C/4 h, 115 °C/4 h	105
OAPS/RDGE	1.0	95 °C/4 h, 115 °C/4 h	115
EVAL F grade[a]			<1.0

[a] Eval F is 32% ethylene−vinyl alcohol copolymer biaxially orientated (3 × 3) and heat-treated to 140 °C.[41]

Table 2. Oxygen Transmission Rates (OTR) of Heat-Pressed Silsesquioxane Films [at 20 °C and 65% RH; cm³ 20 μm/(m² day atm O_2), i.e. Standardized to 20 μm Thickness]

sample	*N* NH_2 groups:epoxide groups	initial curing	curing with pressure	OTR (±0.5) (cm³ 20 μm/(m² day atm))
50% OAPS/PMDA		120 °C/4 h	240 °C/8 h at 1.03 MPa	17
50% OAPS/ODPA		120 °C/4 h	240 °C/8 h at 1.03 MPa	12
50% OAPS/ODPA/ODA		120 °C/4 h	240 °C/8 h at 1.03 MPa	13
OAPS/DGEBA	0.5	120 °C/4 h	200 °C/10 h at 0.690 MPa	7
OAPS/DGEBA	0.5	120 °C/4 h	200 °C/10 h at 0.862 MPa	5
OAPS/DGEBA	0.5	120 °C/4 h	200 °C/10 h at 1.03 MPa	3.9
OAPS/TGMX	0.5	100 °C/1 h, 130 °C/4 h	200 °C/4 h at 1.03 MPa	3.2
OAPS/ECHX	0.5	100 °C/1 h, 130 °C/4 h	200 °C/4 h at 1.03 MPa	5.2
OAPS/TGMX	0.5	100 °C/1 h, 130 °C/4 h	200 °C/4 h at 1.03 MPa	1.2
OAPS/ECHX (i)	0.5	i. 100 °C/1 h 130 °C/4 h	ii. 200 °C/4 h at 1.03 MPa	0.8
OAPS/TGMX (ii)	0.5	ii. 100 °C/1 h		
bilayer		130 °C/4 h		

openings of 40 mm diameter. Mounted films were then placed in the permeation cell and conditioned under steady flow of test and carrier gas for 2 h. Measurements were taken (at ambient humidity) at room temperature, 18, 50, and 70 °C. The 18 °C measurements were achieved by submerging the permeation cell in an ice bath while measurements at 50 and 70 °C were taken with the permeation cell heated in a temperature-controlled oven.

The gas (oxygen) transmission rate P (cm^3 cm cm^2 s cmHg) was obtained by measuring the gas amount q (cm^3) permeated through membrane in time t (s), as follows:

$$t = \frac{60m}{f} \quad \text{(s)}$$

$$P = \frac{ql}{at \times 76} \quad (\text{cm}^3\ \text{cm}/(\text{cm}^2\ \text{s cmHg}))$$

where m is the volume of gas sample loop (cm^3), f the gas flow rate (cm^3/min), q the volume of permeated O_2 gas (cm^3), a the area of membrane (cm^2), and l the thickness of the membrane (cm). Three separate GC measurements (within ±5%) were recorded for each film and averaged. The gas amount q was determined from a calibration curve. The oxygen transmission rate (P) was calculated and standardized to 20 μm thickness. The OTR of the measured films are reported in Tables 1 and 2.

Synthetic Methods and Sample Curing Studies. *TCHS*. OHS, 25.0 g (196.6 mmol of Si−H), and 178.6 mg of PtO_2 were placed in a 500 mL Schlenk flask equipped with magnetic stirrer and condenser. The flask was evacuated and flushed three times with N_2. Toluene (200 mL) and 9.08 mL (122.8 mmol) of 4-vinyl-1-cyclohexene were added via syringe. The reaction mixture was heated at 85 °C for 24 h. The solid PtO_2 catalyst was separated over celite, and residual toluene was removed under vacuum to reveal a white powder (30.9 g, 88%).

Curing TCHS (2.0 g) was placed in a round Teflon Petri dish and heated at temperatures specified in Table 1 to give a 0.4 mm thick film used in gas transport measurements.

OAPS/PMDA Imide Films. OAPS, 25.0 g (173.6 mmol of NH_2−phenyl), was dissolved in 110 mL (1.13 mol) of NMP. This solution was added to another solution containing 18.9 g (86.8 mmol) of PMDA in 100 mL of NMP. The combined solution was stirred at room temperature for 5 min. An 8.0 g portion of solution was cast into molds and heated at temperatures specified in Tables 1 and 2 to give 0.50 mm thick films.

OAPS/ODA/PMDA Imide Films. OAPS (6.25 g, 43.4 mmol of NH_2−phenyl) and ODA (4.35 g, 43.4 mmol of NH_2−phenyl) were dissolved in 110 mL of NMP. This solution was added to another containing 18.9 g (86.8 mmol of anhydride) of PMDA in 100 mL of NMP cooled to 0 °C. The combined solution was stirred at room temperature for 5 min. An 8.0 g portion of solution was cast into molds and heated at temperatures specified in Tables 1 and 2 to give 0.50 mm thick films.

OAPS/ODA/ODPA Imide Films. OAPS (6.25 g, 43.4 mmol of NH_2−phenyl) and ODA (4.35 g, 43.4 mmol of NH_2−phenyl) were dissolved in 110 mL of NMP. This solution was added to another containing 13.5 g (86.8 mmol anhydride) of ODPA in 100 mL of NMP cooled to 0 °C. The combined solution was stirred at 0 °C

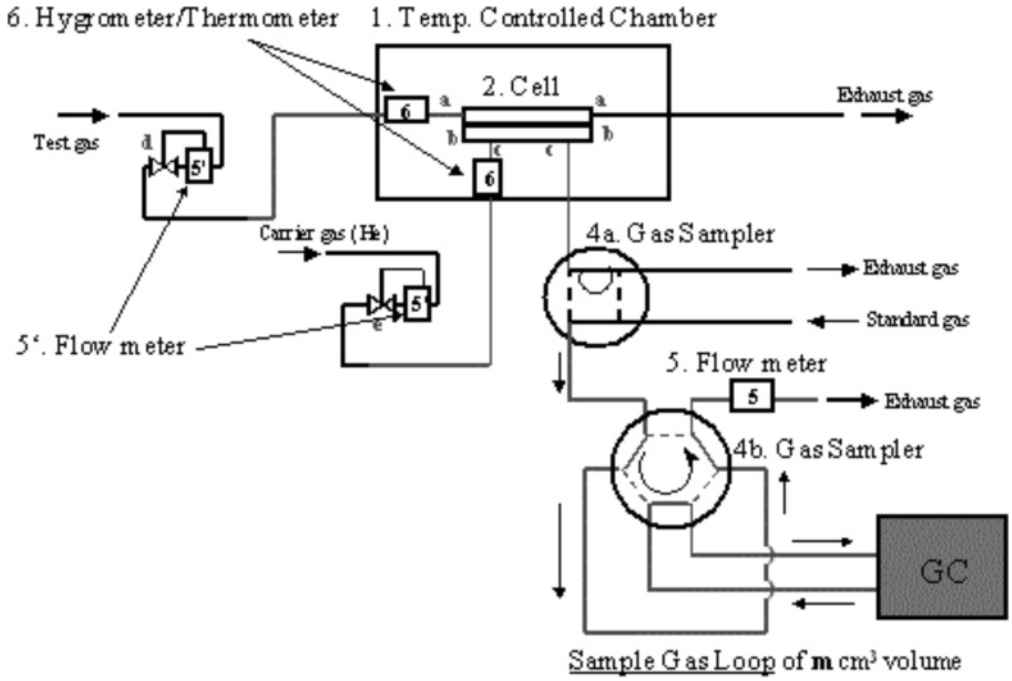

Figure 2. Schematic of GC/permeation cell for determination of OTR (measurements taken at ambient humidity with HP model 5890 series 2 GC).

for 5 min. An 8.0 g portion of this solution was cast into molds and heated at temperatures specified in Tables 1 and 2 to give 0.50 mm thick films.

OAPS/DGEBA Epoxide Films. OAPS (25.0 g, 173.6 mmol NH_2−phenyl) was dissolved in 110 mL of NMP. This solution was added to another solution containing 32.12 g (173.6 mmol of epoxy) of DGEBA in 100 mL of NMP cooled to 0 °C. The combined solution was stirred for 5 min. A 6.0 g portion of solution was cast into molds and heated at temperatures specified in Tables 1 and 2 to give 0.45 mm thick films.

OAPS/ECHX Epoxide Films. OAPS (3.20 g, 22.22 mmol of Ph−NH_2) and ECHX (5.61 g, 44.44 mmol of epoxy) were dissolved in 20 mL of DMF and stirred for 5 min. The solution was cast into molds and heated at temperatures specified in Tables 1 and 2 to give 0.50 mm thick films.

OAPS/TGMX Epoxide Films. OAPS (3.20 g, 22.22 mmol of NH_2) and TGMX (2.29 g, 51.46 mmol of epoxy) were dissolved in 40 mL of THF and stirred for 5 min. The solution was left overnight at room temperature to evaporate THF. The solution was cast into molds and heated at temperatures specified in Tables 1 and 2 to give 0.50 mm thick films.

Warm-Pressed OAPS/TGMX-OAPS/ECHX Bilayer Epoxide Films. OAPS/TGMX films were prepared as above. The films were partially cured at 100 °C/1 h and 130 °C/4 h, after which it became a flexible solid. OAPS/ECHX films were prepared as above and cast onto the partially cured OAPS/TGMX films. Both layers were again heated at 100 °C/1 h and 130 °C/4 h, removed from the mold, sandwiched between aluminum foil sheets, and warm-pressed at 1.03 MPa, as specified in Table 2.

OAPS/RDGE Resin Films. OAPS (3.20 g, 22.2 mmol of $PhNH_2$) and RDGE (4.93 g, 44.4 mmol of epoxy) were dissolved in 40 mL of DMF and stirred for 5 min. The solution was cast into molds and heated at temperatures specified in Tables 1 and 2 to give 0.50 mm thickness films.

Results and Discussion

As noted above, traditional barrier materials rely on close packing of polymer molecules coupled with the introduction of both organic and inorganic crystalline second phases as micro- and nanocomposite barriers within a standard polymer matrix. Given that octafunctional silsesquioxane cages offer the potential to produce very highly cross-linked materials wherein the silica cage not only acts as the cross-linker but also provides a completely dispersed and highly impermeable inorganic phase,[40] the initial goal in this work was to form very short but highly cross-linked materials. Both the epoxy resins of our CTE studies and some of the polyimides studied earlier offer such opportunities.[18,19,22]

In addition, we were also interested in a novel self-curing oligomer that offers the additional potential of relatively high-temperature stability and high hydrophobicity. Thus, we briefly examined the barrier behavior of tetrethylcyclohexenylsilsesquioxanes (TCHS) produced via reaction 3 of Scheme 2. TCHS melts at 120 °C and cures at 180 °C (reaction 4, Scheme 2) to give fully dispersed and transparent materials that show no evidence of nanoporosity by BET. TCHS can be cast as a liquid and cured to provide high-quality films. Unfortunately, as shown below, it is highly permeable to O_2 but may offer utility for separation of other gases. Thus, the majority of the work reported here maps structure−processing−property relationships of silsesquioxane epoxy and imide nanocomposites as O_2 barrier materials. The types of epoxy compounds studied are shown in Figure 3. The oxygen transport values (OTR—measured as a function of film thickness per unit surface area) and curing conditions are shown in Table 1. We have also characterized these materials via a number of standard techniques (see Experimental Section).

In general, the OTR of the films decreases with increasing curing temperatures and times. However, the limiting factor was increased brittleness at higher temperatures, as films cast from solution fractured easily from stresses as they expanded against the molds during curing. In contrast, warm pressing minimized brittle fracture and had a profound effect on barrier properties.

Solution-Cast Films. *TCHS*. Films were formed by curing TCHS per conditions described in Table 1. TCHS is self-curing (reactions 3 and 4); films are completely transparent and have high thermal stability. The 5% mass loss temperature ($T_{d5\%}$) of TCHS is 325 °C, making it ideal for electronics encapsulation. Qualitatively, films have a range of flexibility depending on

Scheme 2

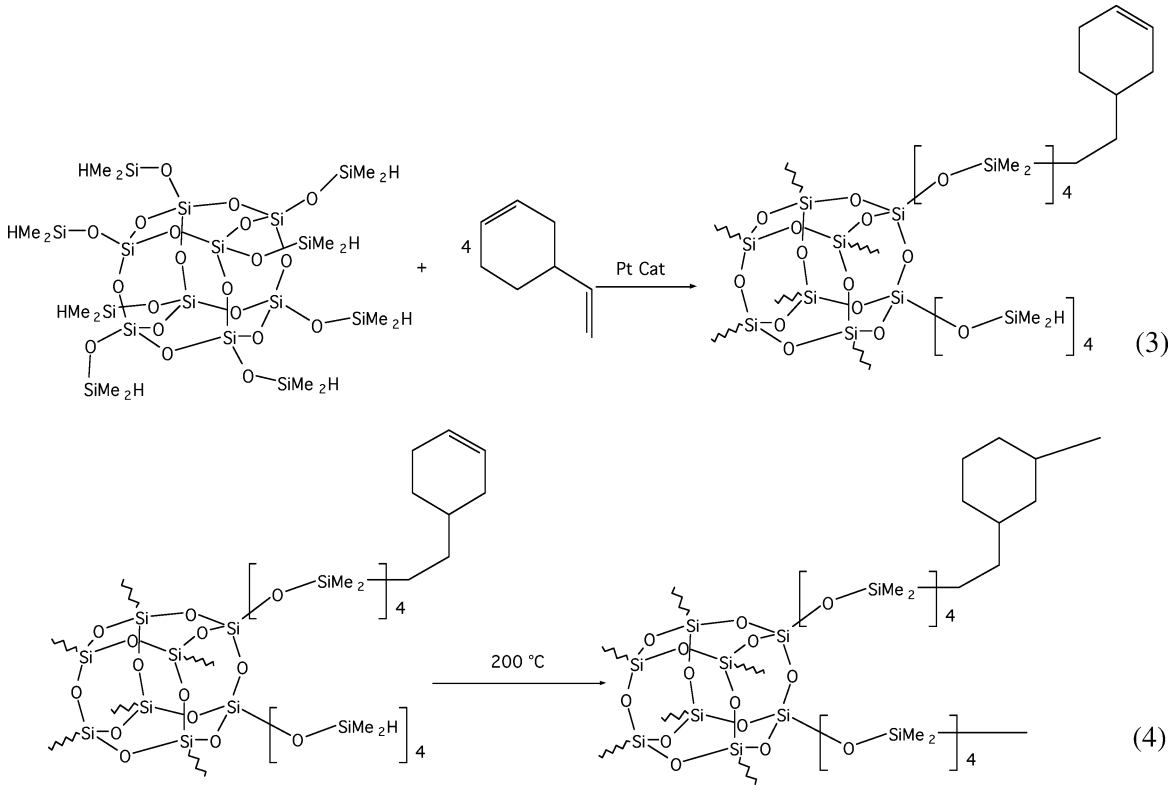

(3)

(4)

the temperature and duration of curing. However, no quantitative measurements of flexibility were made. Films cured at 5 h (170 °C) provided the best flexibility and least color while those subjected to stepwise curing (130 °C/6 h, 130 °C/8 h, 150 °C/8 h, 170 °C/8 h) were most rigid and deeply yellow, yet still transparent. The yellow color comes in part from the retained Pt catalyst.

TCHS was initially synthesized using Pt(dcp), a soluble catalyst, which is quenched after the reaction with PPh_3. However, we speculated that the presence of residual PPh_3 inhibited complete curing of TCHS, explaining the unusually high OTR values recorded in Table 1. According to solid-state NMR studies, 130 °C/5 h and 170 °C/5 h TCHS films are 69% and 79% cured.[40] In response to this, we examined PtO_2-catalyzed hydrosilylation and filtered off the solid catalyst while eliminating the need for PPh_3. While the OTR values using PtO were lower by approximately half (13 000 vs 24 000 cm^3 20 $\mu m/(m^2$ day atm)), they were not as low as expected or desired. Thus, we focused on the polyimide and epoxy systems.

Polyimide Films. We previously described the synthesis, processing, and mechanical properties of two polyimide nanocomposite systems, OAPS/PMDA and OAPS/ODPA.[18,19] Although the OAPS/PMDA materials are very brittle, we were able to successfully process a number of films suitable for OTR measurements. Note that in our earlier studies these materials cured most effectively on heating to ≥300 °C.

As expected, the barrier performance of these films improved with higher temperature (more complete) curing, but cast OAPS/

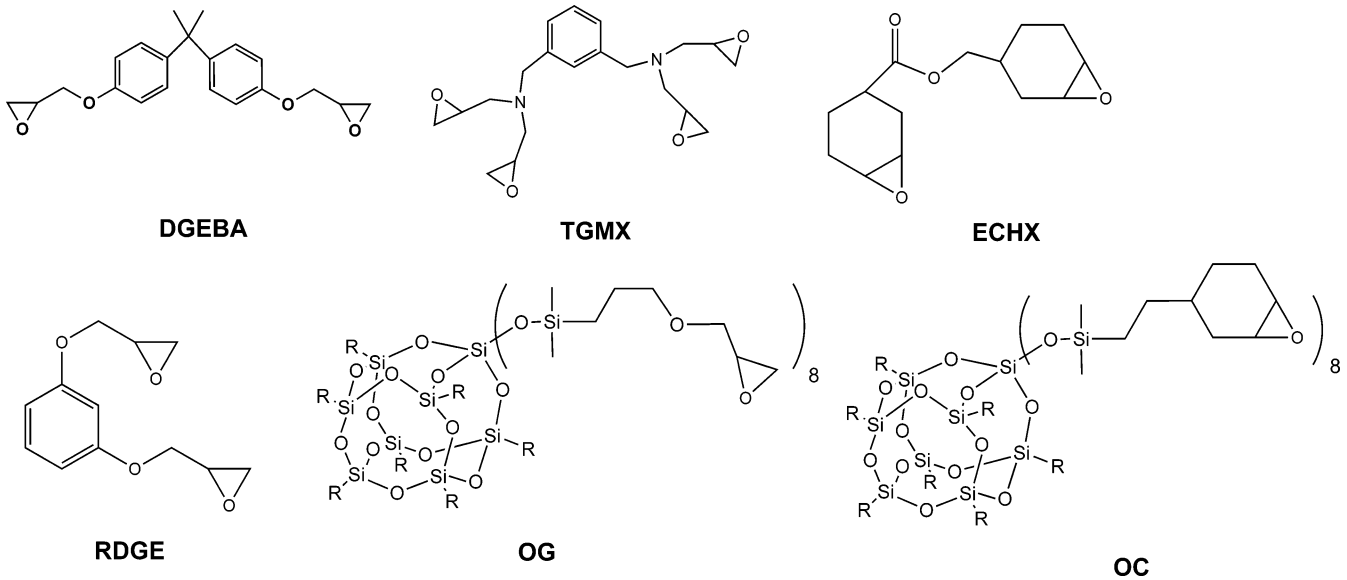

Figure 3. Sets of epoxies tested with various amine curing agents.

PMDA films could not be heated above 240 °C without fracturing into unusable fragments. Even so, films heated stepwise (to minimize cracking) 120 °C/4 h, 205 °C/4 h, 215 °C/8 h, 225 °C/8 h exhibited promising barrier properties (Table 1; 27 ± 0.5 cm^3 20 $\mu m/(m^2$ day atm)) where commercial, biaxially stretched hot and oriented EVAL offer transport values of 1 ± 0.005 cm^3 20 $\mu m/(m^2$ day atm). Note that these values are far superior to those obtained for TCHS and reflect the length (~1.8 nm) and rigidity of the tethers that join the vertices of two cubes.[18,19]

We also measured the barrier properties of analogous OAPS/ODPA films, which also exhibited barrier properties directly related to the degree of curing. Again, while cast OAPS/ODPA samples could not be heated directly to ≥225 °C without cracking, samples cured stepwise to that temperature showed barrier properties (25 cm^3 20 $\mu m/(m^2$ day atm)) competitive with commercial PVA films (20 cm^3 20 $\mu m/(m^2$ day atm))[41] but offering air stability to 550 °C when fully cured. In contrast, the decomposition temperatures of PVA films are very close to their melting temperatures (between 150 and 250 °C), which in turn are dependent on the degree of hydrolysis.[42]

In order to make the films more flexible with the goal of curing to higher temperatures, we introduced ODA (3) as a diluent in the OAPS/ODPA systems. Reactions of equal stoichiometric amounts of OAPS and ODPA with ODA gave films that were much less brittle than undiluted films, with comparable oxygen permeabilities (29 cm^3 20 $\mu m/(m^2$ day atm) for OAPS/ODPA/ODA and 25 cm^3 20 $\mu m/(m^2$ day atm) for OAPS/ODPA) under identical curing conditions (120 °C/4 h, 205 °C/4 h, 225 °C/8 h, 225 °C/8 h).

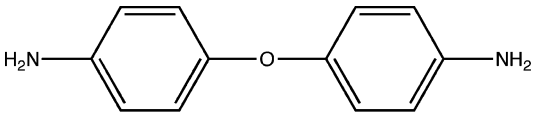

ODA (3)

As Table 1 shows, the use of ODA gives essentially the same barrier performance. However, the resulting films are qualitatively more flexible and also can be cured to somewhat higher temperatures (240 °C) before failure.

Epoxy Resin Films. The bulk of our study focused on OAPS/epoxy resin systems, since they offer the potential for very high chain (cross-link) densities with strong hydrogen bonding as well as the incorporation of an inorganic silica core. Figure 3 provides a complete list of epoxy compounds studied and their structures.

The flexibility of OAPS/epoxy films also depended on cure time and temperature. In general, OAPS/TGMX films were more flexible compared to the other epoxide films at the same curing conditions. All of the transparent films were colored from light yellow to dark orange. OTR values for OAPS/epoxy films exhibited the best properties of all the cast films studied, with OAPS/ECHX (100 °C/1 h, 130 °C/4 h, 180 °C/4 h) exhibiting the lowest OTR (6 cm^3 20 $\mu m/(m^2$ day atm)) observed.

Again, barrier properties generally improved at higher temperatures and longer cure times. For example, O_2 permeability for OAPS/DGEBA (130 °C/5 h) falls from 110 to 21 cm^3 20 $\mu m/(m^2$ day atm) when heated for 5 h more at 150 °C. In addition, these films also benefit from the heat capacity of the silica framework and the ability of the cube to control polymer (tether) chain motion at elevated temperatures. For example, the $T_{d5\%}$ of OAPS/DGEBA is 180 °C, compared to 165 °C for DGEBA alone. However, RDGE films did not offer the same barrier performance as ECHX, DGEBA, or TGMX. While it can be predicted that higher temperature curing may be necessary to reduce the O_2 permeability of OAPS/RDGE films, these films could not be heat treated higher than 115 °C without cracking. Since the epoxide functionalities of RDGE are *meta* to each other across the aromatic ring and because of its relatively short length (compared to DGEBA and TGMX), there might not be enough flexibility in the tethers to limit cracking. Moreover, the ability of the ECHX cyclohexyl epoxides to adopt flexible chair conformations could explain why OAPS/ECHX films do not crack under similar curing conditions to those used for OAPS/RDGE.

We also manipulated the ratio "*N*" (NH_2 groups:epoxide groups) in OAPS/epoxide films to measure the effects on OTR values. In general, a lower *N* value led to improved OTR performance, which corresponds to an increase in cross-link density. The materials with $N = 1.0$ and $N = 0.5$ stoichiometries are most important here because these are the ratios that can give perfectly matched curing to form one or two cross-links per each vertex, respectively. For example, OAPS/ECHX impermeability improves from 24 to 8 cm^3 20 $\mu m/(m^2$ day atm) under the same conditions (100 °C/1 h, 130 °C/4 h) when the *N* ratio is changed from 1.0 to 0.5, respectively.

Warm-Pressed Films. While "cube" films exhibit excellent barrier properties when cast from solution, warm pressing dramatically lowers the OTR of the OAPS/imide and epoxide films (see Table 2). Initially, the films are precured (Table 2) to remove solvent and then cured under pressure between heated platens (see experimental details). Note that Table 2 conditions represent maximum temperatures and loads during curing; higher temperatures and pressures cause films to crack.

There is significant improvement in the barrier properties of both OAPS/imide and epoxide systems when cured under pressure. It is reasonable to assume that heating under pressure eliminates voids and pores resulting from residual solvent eliminated in the procuring step.

This is not unexpected given that it is known that a combination of heat treatment and orientation will improve gas barrier properties in ordinary polymer films, but improvement by orientation alone without heat treatment is usually marginal.[41] This suggests that thermal treatment of film systems has a direct influence on chain−chain ordering (crystallinity), which determines the performance of barrier films. Heat treatment under pressure may allow the cubes and tethers to order under conditions where they usually do not crystallize. Future powder XRD studies could elucidate whether or not this is the case.

The improvement in the polyimide films was significant, but not as dramatic as for the epoxide systems. The OTR of OAPS/TGMX films, for example, drops from 14 (as cast) to 3.2 when cured at 1.03 MPa. Warm pressing reduces the propensity of films to crack, permitting higher cure temperatures. In addition, the curing times for all systems are shortened without sacrifice to barrier performance.

A bilayer of OAPS/TGMX and OAPS/ECHX film cured under pressure exhibits the best OTR of the cube films, 1.2 cm^3 20 $\mu m/(m^2$ day atm). We have obtained values as low as ≈0.8 cm^3 20 $\mu m/(m^2$ day atm) for this same system but are hindered by the detection limits of our instrumentation, and thus these systems may actually be better than we are currently able to report. The transparent dark purple bilayer film offers excellent adhesion between the layers. Unfortunately, efforts to form OAPS/DGEBA bilayers with OAPS/TGMX or OAPS/ECHX were not possible due to delamination after curing. More work and the possibility of making tri- and tetralayer films offer further potential to improve barrier properties. In addition, it may be possible to spray coat the individual layers since these

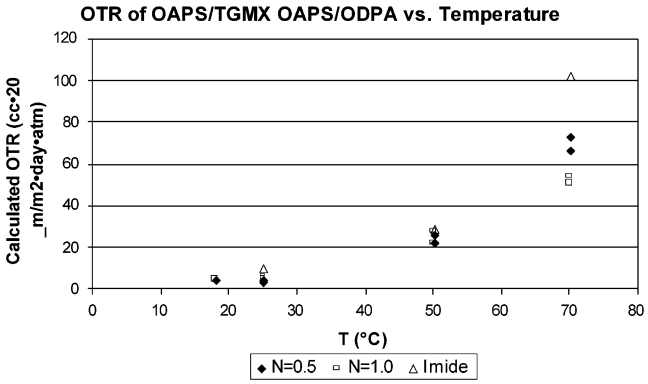

Figure 4. OTR vs temperature: OAPS/TGMX (100 °C/1 h, 200 °C/4 h at 150 psi) and OAPS/ODPA (120 °C/4 h, 275 °C/8 h at 150 psi). $E_a \approx 10 \pm 2$ kcal.

materials will cure near room temperature.

Temperature Dependence. The dependence of OTR on temperature was investigated for OAPS/TGMX and OAPS/ODPA (Figure 4), as they represent the most flexible epoxy and imide films that still maintain excellent barrier properties.

As expected, the permeability of each film increases at temperatures above room temperature due to increased molecular motion of polymer segments in these films even though they rarely exhibit significant T_gs. Conversely, at lower temperatures the decreased motion of these segments improves OTR. In addition, the temperature-dependent asymptotic decrease in permeability is also attributed to the corresponding decrease in kinetic energy of the permeating O_2 molecules at lower temperatures.[43]

At room temperature, the majority of epoxide films with $N = 0.5$ exhibit better barrier performance while films with $N = 1.0$ perform better at higher temperatures. This suggests that the increased cross-link density for OAPS/TGMX films improves OTR but only at low temperatures. The decrease in barrier performance at elevated temperatures, however, may be attributed to both a significant increase in motion of the permeant gas and the organic tethers, which leads to increased O_2 transport. This suggests that a high degree of cross-linking is unfavorable since any significant increase in tether motion could lead to nanosized cracks in the films.

At $N = 1.0$, the degree of cross-linking is essentially halved, and the film may be able to relieve any strain caused by motion via flexing at the molecular level. This strain relief may explain why polyimide films behave relatively poorly at elevated temperatures due to the short length and rigidity of cross-linking units. At lower temperatures, however, increased cross-link density is not a problem due to both the decreased motion of the tethers and lower gas mobility.

Since increased cross-link density improves OTR performance at temperatures <50 °C yet presents a liability at higher temperatures, it may be possible to tailor these films across a broad temperature range by maintaining maximum cross-link density with longer and somewhat more flexible epoxy tethers. Theoretically, these systems should present the same barriers to oxygen permeation at lower temperatures while decreasing OTR at increased temperatures by flexing to avoid strain that leads to cracking. It could also lead to easier processing and perhaps the opportunity to align tethers through uniaxial or biaxial stretching.

Conclusions

We have found that OAPS/imide and OAPS/epoxide films exhibit excellent barrier properties, competitive with current commercial grade barrier films.[41] While cast OAPS/ODPA and OAPS/ECHX epoxide films have promising OTRs of 25 and 6 cm^3 20 μm/(m^2 day atm) (at optimum curing conditions), a significant improvement is achieved with warm pressing. A combination warm-pressed, bilayer film system consisting of OAPS/ECHX and OAPS/TGMX was found to have OTR of <1 cm^3 20 μm/(m^2 day atm). It should be noted that commercial barrier films with similar performance are usually achieved with three or four different film layers and may utilize adhesives to keep the films together.[44]

The structures of the organic tethers, as well as cross-link densities, determine O_2 permeability. Long and flexible organic tethers improve the film's overall flexibility, an important factor during warm pressing. While increasing cross-link density traditionally improves OTR, high cross-link density of short and stiff tethers leads either to cracking during curing or nanosized cracks or more free volume at elevated temperatures for reasons stated above. At low temperatures, however, the movement of short and stiff tethers is minimized and high cross-link density improves OTR. We have determined that the ideal silsesquioxanes film would have a high cross-link density of long, flexible tethers to achieve maximum performance at a wide range of temperatures.

Silsesquioxane films, particularly OAPS/imide and OAPS/epoxide films, provide excellent O_2 barrier properties potentially of use for a wide variety of packaging applications. The silsesquioxanes films can in principle be further functionalized to tailor barrier properties or for selected transport of specific gases for separation applications. It was recently demonstrated both theoretically and experimentally that silsesquioxanes offer higher barriers to N_2 diffusion than O_2.[40] They also offer high thermal stability of potential use in high-temperature applications such as electronics packaging.

Note that our results contrast considerably with polysiloxane films, which are well-known to have high oxygen permeabilities (>19 000 cm^3 20 μm/(m^2 day atm)) due to the high degree of chain flexibilities.[44] Consequently, our results again support the utility of using nanoscale tailoring with nanoscopic silsesquioxane units to closely control global properties.

Acknowledgment. We thank NSF IGERT and in particular Kuraray Ltd. for support of this work.

References and Notes

(1) Kamat, P. V. *J. Phys. Chem. B* **2002**, *106*, 7729.
(2) Champion, Y., Fecht, H.-J., Eds. *Nano-Architectured and Nanostructured Materials: Fabrication, Control and Properties*; Wiley-VCH: Weinheim, 2005.
(3) Wang, Z. L., Liu, Y., Zhang, Z., Eds. *Handbook of Nanophase and Nanostructured Materials*; Kluwer Academic/Plenum Publ: New York, 2002; Vol. 3.
(4) Shen, Y.; Friend, C. S.; Jiang, Y.; Jakubczyk, D.; Swiatkiewicz, J.; Prasad, P. N. *J. Phys. Chem. B* **2000**, *104*, 7577.
(5) Davis, M. E.; Katz, A.; Ahmad, W. R. *Chem. Mater.* **1996**, *8*, 1820.
(6) Moriarty, P. *Rep. Prog. Phys.* **2001**, *64*, 297.
(7) Voronkov, M. G.; Lavrent'yev, V. I. *Top. Curr. Chem.* **1982**, *102*, 199.
(8) Baney, R. H.; Itoh, M.; Sakakibara, A.; Suzuki, T. *Chem. Rev.* **1995**, *95*, 1409.
(9) Lichtenhan, J. In *Polymeric Materials Encyclopedia*; Salmone, J. C., Ed.; CRC Press: New York, 1996; Vol. 10, pp 7768−7777.
(10) Provatas, A.; Matisons, J. G. *Trends Polym. Sci.* **1997**, *5*, 327.
(11) Laine, R. M. *J. Mater. Chem.* **2005**, *15*, 3725.
(12) Sellinger, A.; Laine, R. M. *Macromolecules* **1996**, *29*, 2327.
(13) Sellinger, A.; Laine, R. M. *Chem. Mater.* **1996**, *8*, 1592.
(14) Zhang, C.; Laine, R. M. *J. Organomet. Chem.* **1996**, *521*, 199.
(15) Zhang, C.; Babonneau, F.; Bonhomme, C.; Laine, R. M.; Soles, C. L.; Hristov, H. A.; Yee, A. F. *J. Am. Chem. Soc.* **1998**, *120*, 8380.
(16) Zhang, C.; Laine, R. M. *J. Am. Chem. Soc.* **2000**, *122*, 6979.

(17) Tamaki, R.; Tanaka, Y.; Asuncion, M. Z.; Choi, J.; Laine, R. M. *J. Am. Chem. Soc.* **2001**, *123*, 12416.
(18) Tamaki, R.; Choi, J.; Laine, R. M. *Chem. Mater.* **2003**, *15*, 793.
(19) Choi, J.; Tamaki, R.; Kim, S. G.; Laine, R. M. *Chem. Mater.* **2003**, *15*, 3365.
(20) Laine, R. M.; Choi, J.; Lee, I. *Adv. Mater.* **2001**, *13*, 800.
(21) Choi, J.; Yee, A. F.; Laine, R. M. *Macromolecules* **2003**, *15*, 5666.
(22) Sulaiman, S.; Brick, C. M.; De Sana, C. M.; Katzenstein, J. M.; Laine, R. M.; Basheer, R. A. *Macromolecules* **2006**, *39*, 5167.
(23) Kim, G. M.; Qin, H.; Fang, X.; Sun, F. C.; Mather, P. T. *J. Polym. Sci., Part B: Polym. Phys.* **2003**, *41*, 3299.
(24) Ramirez, C.; Abad, M. J.; Barral, L.; Cano, J.; Diez, F. J.; Lopez, F. J.; Montes, R.; Polo, J. *J. Therm. Anal. Calorim.* **2003**, *72*, 421.
(25) Leu, C.-M.; Chang, Y.-T.; Wei, K.-H. *Chem. Mater.* **2003**, *15*, 3721.
(26) Seino, M.; Kawakami, Y. *Polym. J.* **2004**, *36*, 422.
(27) Huang, J. C.; Xiao, Y.; Mya, K. Y.; Liu, X. M.; He, C. B.; Dai, J.; Siow, Y. P. *J. Mater. Chem.* **2004**, *14*, 2858.
(28) Zheng, L.; Farris, R. J.; Coughlin, E. B. *Macromolecules* **2001**, *34*, 8034.
(29) Neumann, D.; Fisher, M.; Tran, L.; Matisons, J. G. *J. Am. Chem. Soc.* **2002**, *124*, 13998.
(30) Pittman, C. U.; Li, G. Z.; Ni, H. *Macromol. Symp.* **2003**, *196*, 301.
(31) Camper, D.; Bara, J.; Koval, C.; Noble, R. *Ind. Eng. Chem. Res.* **2006**, *45*, 6279 and references therein.
(32) Van der Bruggen, B.; Jansen, J. C.; Figoli, A.; Geens, J.; Van Baelen, D.; Drioli, E.; Vandecasteele, C. *J. Phys. Chem. B* **2004**, *108* 13273 and references therein.
(33) Ha, S. Y.; Park, H. B.; Lee, Y. M. *Macromolecules* **1999**, *32*, 2394 and references therein.
(34) Okahata, Y.; Shimizu, A. *Langmuir* **1989**, *5*, 954.
(35) Nishide, H.; Tsukahara, Y.; Tsuchida, E. *J. Phys. Chem. B* **1998**, *102*, 8766.
(36) Wilson, M. A.; Pohorille, A. *J. Am. Chem. Soc.* **1996**, *118*, 6580.
(37) Solovyov, S. E. *J. Phys. Chem. B* **2006**, *110*, 17977.
(38) Sweeny, R. F.; Rose, A. *Ind. Eng. Chem. Product Res. Dev.* **1965**, *4*, 248.
(39) Abe, A.; Albertsson, A.-C.; Duncan, R.; Dusek, K.; Jeu, W. H. D.; Joanny, J. F.; Kausch, H.-H.; Kobyashi, S.; Lee, K.-S.; Leibler, L.; Long, T. E.; Manners, I.; Möller, M.; Nuyken, O.; Terentjev, E. M.; Voit, B.; Wegner, G.; Wiesner, U. *Inorganic Polymeric Nanocomposites and Membranes; Adv. Polym. Sci. No. 179*; Springer: Berlin, 2005.
(40) Tejerina, B.; Gordon, M. S. *J. Phys. Chem. A* **2002**, *106*, 11764.
(41) Takamura, N.; Viculis, L.; Zhang, C.; Laine, R. M., submitted to *Polym. Int.*
(42) Eval Americas Technical Bulletin No. 110, *Barrier Properties of Eval Resins,* 2000.
(43) Mark, J. E., Ed. *Physical Properties of Polymers Handbook*, 2nd ed.; *AIP Series in Polymers and Complex Materials*; AIP Press: Woodbury, NY, 1996.
(44) Hong, S.-I.; Krochta, J. M. *J. Food Eng.* **2006**, *77*, 739.
(45) Massey, L. K. *Permeability Properties of Plastics and Elastomers—A Guide to Packaging and Barrier Materials*, 2nd ed.; William Andrew Publishing/Plastics Design Library: Norwich, NY, 2003.

MA062305P